*International Conference on Mathematics, Computational Methods & Reactor Physics (M&C 2009)*
Saratoga Springs, New York, May 3-7, 2009, on CD-ROM, American Nuclear Society, LaGrange Park, IL (2009)

# DETERMINISTIC AND STOCHASTIC APPROACH FOR A VOID REACTIVITY EFFECT EVALUATION:
application to a Generation IV Lead Fast Reactor (LFR)

**Sara Bortot*, Rasha Ghazy, Marco E. Ricotti**
Politecnico di Milano – Department of Energy
Nuclear Division – CeSNEF
Via La Masa, 34 – 20156 Milano, ITALY
sara.bortot@mail.polimi.it; rasha.ghazy@mail.polimi.it; marco.ricotti@polimi.it

**Carlo Artioli, Vincenzo Peluso, Massimo Sarotto**
FIS-NUC ENEA
National Agency for the New Technologies, Energy and Environment
Via Martiri di Monte Sole, 4 – 40129 Bologna, ITALY
carlo.artioli@bologna.enea.it; peluso@bologna.enea.it; massimo.sarotto@bologna.enea.it

## ABSTRACT

This paper concerns two independent neutronic analyses performed by means of both a deterministic and a stochastic code, with the aim of evaluating the impact of different approaches and numerical methods on the calculation of critical reactor parameters.
With regards to neutronics, the optimization of core design is strongly related to the accurate determination of important quantities as power distributions, absorbers worth and reactivity coefficients.
An aspect of great relevance in Lead Fast Reactors (LFR) is the actual void reactivity evaluation: the purpose of this work is therefore to outline the physical problem and to compare the results concerning void effect contributors through a 'cross-checked' analysis.
The field of investigation assumed for the code comparison corresponds to the reference configuration of the 600 MWe European Lead-cooled SYstem (ELSY-600), one of the Lead-cooled Fast Reactors within Generation IV Nuclear Energy systems program, under investigation in the EU 6$^{th}$ FP.
Analyses are carried out on a 1500 MWth core with typical European mixed oxide fuel (MOX) in a three enrichment zones configuration made of wrapperless subassemblies and pins in square-lattice arrangement.
The deterministic code ERANOS-2.1 and the Monte Carlo MCNP-4a have been employed in conjunction with the updated nuclear data library JEFF 3.1.
ERANOS-2.1 has been utilized to assess the void reactivity variation and its splitting into the most relevant nuclides. Results have been compared with Monte Carlo outcomes of an analogous analysis performed by means of MCNP-4a, in order to get a rough idea of the spread of values for the considered parameters.

*Key Words*: Deterministic, Stochastic, Reactivity, Cross Sections, Void Effect.

## 1. INTRODUCTION

* Corresponding Author

Uncertainties associated with the characterisation of core materials neutronic properties have a significant impact on reactor physics parameters such as power distributions, absorbers worth and reactivity coefficients.

The actual void effect evaluation is a crucial, safety-related issue in Lead Fast Reactors (LFR). Since the amount of reactivity provided by feedback and by the control system must be strictly related to it –and to other transients-, a good estimation of reactivity parameters is required in order to guarantee an effective compensating action against reactivity swings.

In this paper, an effort has been initiated for outlining the physical mechanism involved in LFR coolant voiding, as well as for estimating a range of values for the neutronic parameters affecting the reactivity variation due to void occurrence.
In such a context, the deterministic code ERANOS-2.1 (European Reactor ANalysis Optimized calculation System) in conjunction with JEFF 3.1 nuclear data library has been used to analyse the preliminary core configuration of the European Lead-cooled SYstem (ELSY). It is a pool-type lead-cooled 600 MWe fast reactor, under investigation since September 2006 within the Sixth EURATOM Framework Programme.
The deterministic calculations have been compared with Monte Carlo estimates: results of an analogous study performed by means of MCNP-4a stochastic code have been taken as reference [1], considering that nuclear data uncertainties have a non-negligible impact on design studies and performance parameters [2].
Analyses have first covered the investigation of phenomena occurring during voiding, and then a core-widely evaluation of void reactivity effect has been performed. Finally, variation of fissions, captures and escapes due to voiding has been investigated for each significant isotope composing the fuel.

## 2. ELSY VOID REACTIVITY EFFECT EVALUATION

### 2.1 Voiding Mechanism and Phenomena

Void worth stands as one of the major safety parameters; loss of coolant from the active core in LFRs results in a large positive reactivity effect, which can be formally expressed as the relative change in reactivity per variation in void fraction α:

$$\alpha_v = \frac{1}{k_{\text{eff}}} \frac{\partial k_{\text{eff}}}{\partial \alpha} \tag{1}$$

being

$$\alpha = \frac{Void\ \ Volume}{TotalVolume} = \frac{V_v}{V}, \tag{2}$$

where the '*Total Volume*' is the coolant volume in the unperturbed configuration.
The total coolant void worth of the system is represented by the difference in the *k*-eigenvalue between the flooded and voided state.

In general, the occurrence of void in a core can be a result of many failure events, namely fuel pin rupture and consequent release of fission gases, coolant temperature increase resulting in density changes, steam ingress from ruptured steam generator, blow-up of bubbles from gas injection system.

The physical effects induced by coolant voiding or, more generally, density decreasing in fast cores are:

- spectral hardening due to reduction of neutron moderation;
- increasing fission probabilities of 'even-even' actinides;
- reduction of neutron parasitic absorption in fuel, cladding and coolant;
- increasing leakage.

## 2.2 ELSY Configuration and Parameters Studied

ELSY fast reactor has been modelled in the wrapperless square design option, concerning the preliminary core configuration defined for a 1530 MW thermal power [3].
In particular, a Fuel Assembly (FA) open square design has been obtained by arranging 17 x 17 pins (5 positions of which are devoted to the SS structure) as in usual PWRs. The FA geometrical characteristics with their average working temperatures are schematised in Figure 1.

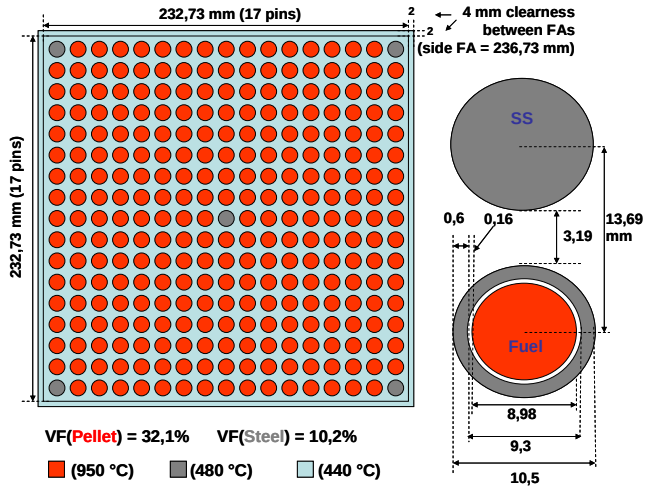


**Figure 1. ELSY Fuel Assembly design (90 cm active height).**

The core contains 272 FAs: 132 in the inner zone with a plutonium enrichment ($PuO_2$ /( $PuO_2$ + $UO_2$) Volume Fraction, VF) of 13.4%, 72 in the intermediate zone with 15.0% (VF) plutonium enrichment, and 68 in the outer one with 18.5% (VF) plutonium enrichment.
Twelve $B_4C$ Control Rods (with 70% VF of $B_4C$, boron 90% enriched in $B_{10}$) have been located between the outer and intermediate fuel zones.

Analyses of reactivity increase due to coolant expulsion have been carried out simulating the voiding of the whole and only active region, while keeping the lead reflector around. Such a configuration has been taken as reference condition notwithstanding the fact it is a non-realistic event. Nevertheless this schematisation allows coherent comparisons and offers an indication of void effect importance.
Such a global void effect can be inferred as consequence of changes on the different contributions to $k_{eff}$, which has been evaluated both core-widely and analysing each region and each fuel isotope contribution.
In the context defined above, the following types of code predictions have been investigated:

- The multiplication factor $k_{eff}$ and its relative variation $\partial k_{eff} / k_{eff}$ :
  comparisons of these integral parameters provide an overall assessment of the accuracy of the calculation methods, as well as a global view of different geometry models.
- The average number of neutrons produced per fission, $\bar{\nu}$:
  this parameter is a valuable spectral effect indicator because of its sensitivity to spectrum shifting; it has been evaluated both globally and for each nuclide in each core region in order to have local indications.
- Fission and Capture Rates:
  these reaction rates depend markedly on both neutron flux and spectrum: in particular, variations in uranium 238 fission cross section due to spectral hardening (threshold reactions) are expected to play a relevant role in void reactivity worth.

## 3. GEOMETRY MODELS

The whole area of interest has been studied and because of the theta-symmetry of the problem a homogenized reactor *R-Z* model has been first constructed to perform neutron transport calculations.

Such a model has been set up in cylindrical geometry and includes ten regions, presented in Figure 2, with the reactor core and blanket components being homogenized. The radius of the model is 290 cm and the height is 450 cm (cold dimensions).

The spatial meshing adopted is non-uniform in both the radial and the axial directions: the first one is characterized by a $\Delta R$ of the order of 2÷3 cm, while the second is coarser ($\Delta Z$~10 cm), except for the active zone, in which the mesh is refined up to 2÷2.5 cm.

Average steady-state temperatures have been assumed: 950°C for the fuel, 480°C for pin clad and structural pins, 440°C for coolant and steel structures.

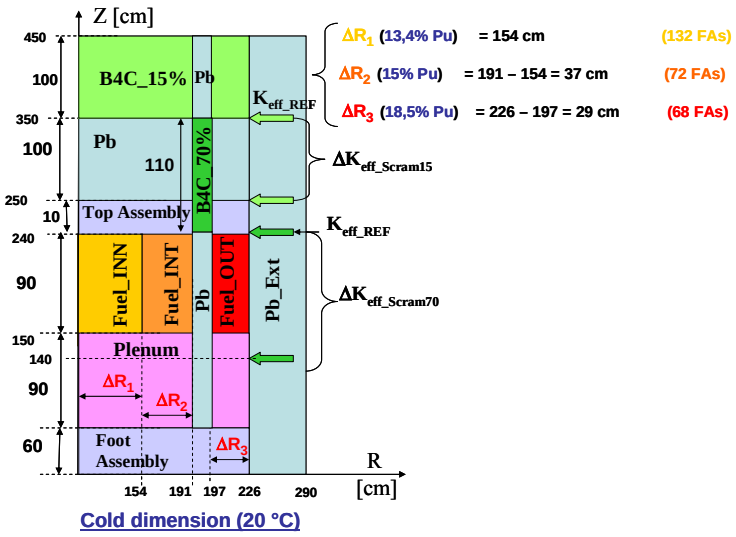


**Figure 2. 1530 MWth ELSY equivalent *R-Z* model (cold dimensions).**

Then, a tri-dimensional reactor model has been set up: a quarter of the core has been modelled assembly by assembly with null-derivative boundary conditions for the $X$ and the $Y$ inferior limits and vacuum elsewhere (all neutrons reaching the surface are considered escaping from the system).

A uniform coarse meshing has been adopted in both the $X$ and the $Y$ directions ($\Delta X=\Delta Y \sim 20$ cm) and a subsequent refinement has been applied ($\Delta X=\Delta Y \sim 10$ cm).

As to the axial direction, a same discretization has been maintained in the two cases: the active region is described by a mesh of the order of 10 cm, while other zones, judged as less important with respect to the void reactivity worth, have been modelled with a coarser mesh ($=\Delta Z \sim 20$ cm).

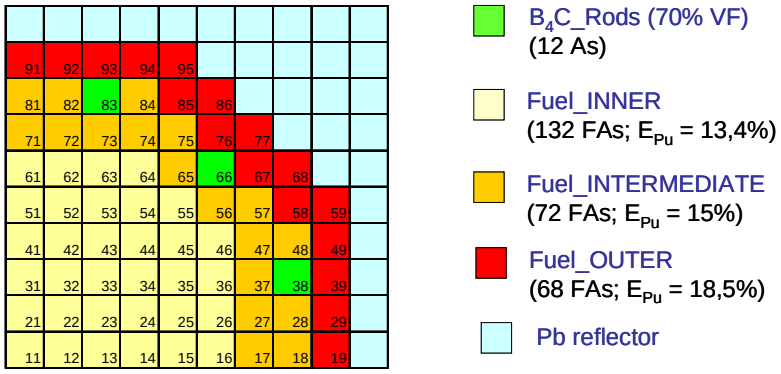


**Figure 3. 1530 MWth ELSY 3D core design.**

It is pointed out that a homogeneous-zone core configuration is assumed in all bi-dimensional and tri-dimensional cases. In this context, core heterogeneity might alter the coolant void

reactivity significantly. Monte Carlo codes are not affected by this kind of approximations thanks to their point-wise spatial description, which is in accordance with the real physical system.

## 4. NEUTRON TRANSPORT CALCULATIONS

Deterministic and Monte Carlo methods are two distinct approaches that have been developed for several decades in order to solve the neutron transport problem.

Depending on the matter characteristics, each method presents advantages and weaknesses. Furthermore, there are many possible uncertainties associated with phase-space discretization and numerical options that are inherent in multigroup $S_N$ and nodal methods.

On the other hand, continuous-energy Monte Carlo simulations are relatively straightforward in both physics and geometry modelling. Therefore, Monte Carlo results have been regarded as referential and deviations of $S_N$ and nodal outcomes have been evaluated.

### 4.1 Deterministic Computational Schemes

Deterministic methods require the solution of the Boltzmann equation governing the neutron population distribution. ERANOS code (version 2.1) separates the problem solving in two parts: firstly, cross-sections and matrices have been prepared by the cell/lattice code ECCO for a given number of energy groups and for an equivalent homogeneous medium corresponding to the cell. Then the core calculation has been performed by using 33-groups cross sections to determine reactor characteristics, as the flow chart in Figure 4 shows [4].

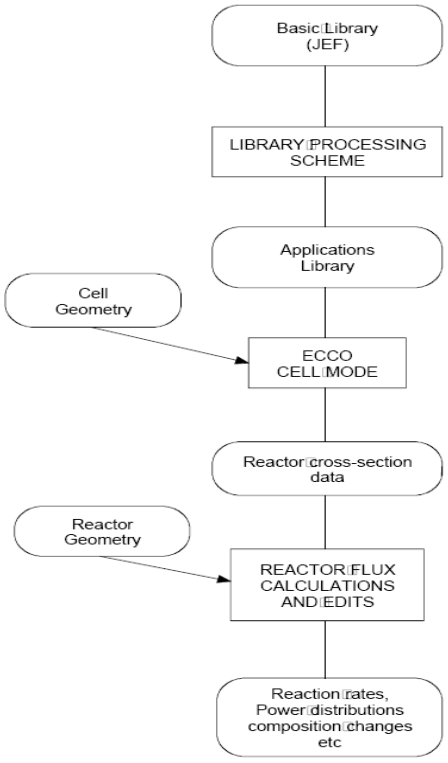


**Figure 4. ERANOS processing route.**

This separation corresponds to a two-level description of the reactor geometry, and its limitation consists in the breakdown of the assumption of a zero net current at the outer boundary of the cell.

When comparing the results of multigroup and continuous-energy evaluations, the multigroup cross section library choice usually plays an important role; for this reason, criticality calculations have been performed by ERANOS-2.1 with use of JEFF 3.1 multigroup cross section library, which is the same adopted in the reference Monte Carlo analysis.

### 4.1.1 Discrete ordinates calculations

Spatial estimates have been carried out by the ERANOS module BISTRO (BI-dimensional $S_N$ TRansport Optimisé) -which solves the transport equation by using a discrete ordinates-coarse mesh and finite differences- in the cylindrical *R-Z* bi-dimensional model.
Computational costs of the $S_N$ method are generally negligible compared to those of the analogous Monte Carlo calculation. However, execution of the $S_N$ method inevitably invokes discretization on spatial, angular and energy variables.

### 4.1.2 Nodal calculations

The OECD version of the variational nodal method developed for the VARIANT code has been used in ERANOS-2.1 as the TGV/VARIANT module. This method is based on the second-order form of the even-parity transport equation. A solution is searched in form of expansions for the even and odd parity fluxes in pre-computed angular and spatial basis functions with unknown coefficients. These basis functions correspond to orthogonal polynomials for the spatial variables and spherical harmonics for the angular variables. Scattering anisotropy can be taken into account as $P_N$ moments up to the order $N$ of the Legendre expansion of the flux. A 'simplified transport' option exists, in which the angular developments both within the nodes and at the node boundaries are truncated by neglecting high-order cross terms. This option is rather accurate in practice (large reactors), and less time and memory consuming.
In the present work a summary evaluation of the impact of the mesh size for spatial discretization and of the Legendre expansion order of multigroup cross sections has been done: flux calculations have been performed either setting the simplified spherical harmonics treatment option, or representing the scattering cross section with the $P_{0\text{-corrected}}$ and $P_1$ Legendre polynomial expansion, or with both a coarse and a more refined mesh.

The Monte Carlo code MCNP version 4a with the JEFF3.1 library has been applied to work out the same issue. Arrangement of geometry and materials are modelled identically as in nodal calculations.

## 5. RESULTS AND COMPARISONS

This section presents the results of the numerical investigations carried out.
Firstly, the overall performance of the different deterministic options is assessed by comparing predictions of the neutron multiplication factor $k_{eff}$ and of its differential between the reference and the voided configuration.
Specific comparisons are then made over void significant parameters and reaction rates: in each case, results of deterministic calculations are compared to Monte Carlo simulations.

### 5.1 Deterministic Evaluations of the Neutron Multiplication Factor $k_{eff}$

Criticality results of different deterministic calculations performed over bi-dimensional and tri-dimensional geometry models are next illustrated and compared.
Figure 5 shows that $k_{eff}$ varies from a minimum of 0.98957 to a maximum of 0.99549 for the reference configuration, and from a minimum of 1.04207 to a maximum of 1.04926 for the voided configuration. Therefore, the worse excursion range this parameter is determined with is of the order of 700 pcm.
Despite these discrepancies in the absolute values of $k_{eff}$, a correlation is observed between individual reference and perturbed couple-values: systematic errors in over-estimating or under-estimating $k_{eff}$ actual values occur both in the reference and in the perturbed calculations. As a consequence of this kind of ‘first order’ compensation, differentials are less sensitive to

code/geometry variability: they lie within a total spread of about 170 pcm, varying from $\Delta k_{eff}$ = 0.05209 to $\Delta k_{eff}$ = 0.05377 respectively (Figure 6).
The concerning total void reactivity worth turns out to be $\Delta\rho$ = 5039 pcm and $\Delta\rho$ = 5171 pcm.
A finite differences diffusion calculation has been carried out as a check trial on the bi-dimensional *R-Z* geometry, and a fairly good agreement with transport results has been noticed: the void reactivity worth turns out to be $\Delta\rho \sim 4700$ pcm, which is a good result considering differences between transport and diffusion treatments.

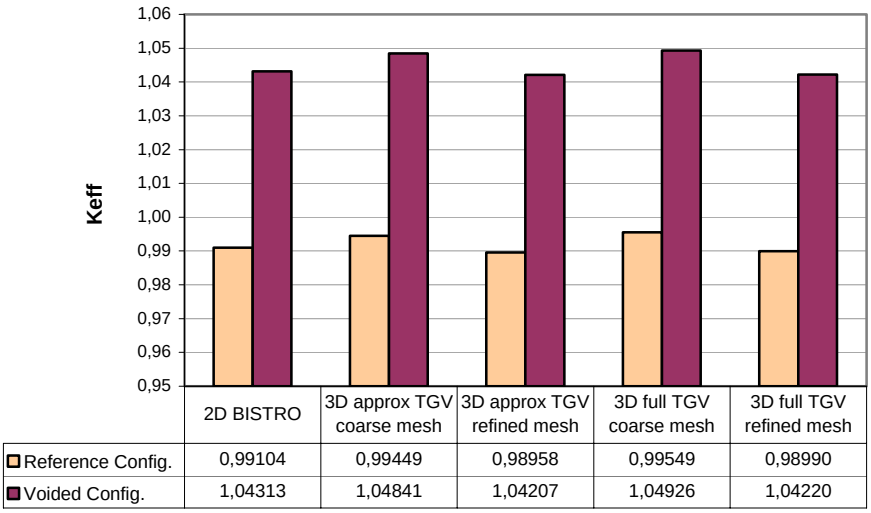


| | 2D BISTRO | 3D approx TGV coarse mesh | 3D approx TGV refined mesh | 3D full TGV coarse mesh | 3D full TGV refined mesh |
|---|---|---|---|---|---|
| Reference Config. | 0,99104 | 0,99449 | 0,98958 | 0,99549 | 0,98990 |
| Voided Config. | 1,04313 | 1,04841 | 1,04207 | 1,04926 | 1,04220 |

**Figure 5. Deterministic results on $k_{eff}$ before and after occurrence of void.**

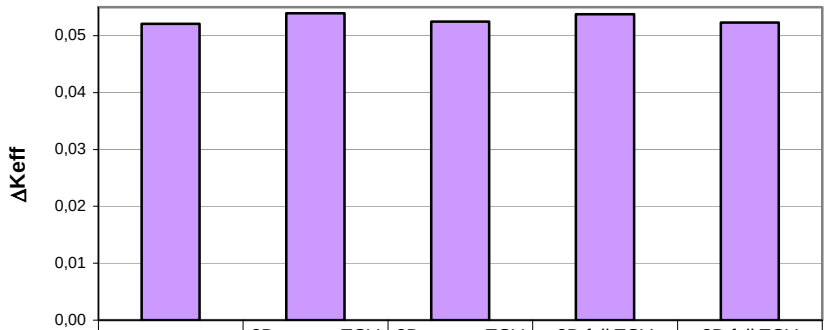


| | 2D BISTRO | 3D approx TGV coarse mesh | 3D approx TGV refined mesh | 3D full TGV coarse mesh | 3D full TGV refined mesh |
|---|---|---|---|---|---|
| Delta K | 0,05209 | 0,05392 | 0,05249 | 0,05377 | 0,05230 |

**Figure 6. Deterministic evaluations of $\Delta k_{eff}$ between voided and reference configuration.**

Therefore it can be concluded that the reactivity effect investigated (namely the effect of core voiding) enjoys a kind of stability with respect to the computational schemes adopted.

Being interested in *deltas* between a reference and a perturbed condition, the choice of a more or less accurate geometry description and computational models turns out to be not so impacting.

## 5.2 Void Reactivity Worth Evaluation

Results of $k_{eff}$ predictions are shown in Figure 7: deterministic values corresponding to the less accurate geometry description (cylindrical *R-Z* model) and the most refined one (3D, refined mesh) are compared with reference MCNP results.
The graph clearly shows a good agreement between 2D and 3D calculations, on the basis of which ELSY void effect accounts for 5039 and 5069 pcm respectively.
All the deterministic calculations underestimate the total void reactivity worth to some extent compared with the Monte Carlo results of $\Delta\rho$= 5234 pcm.

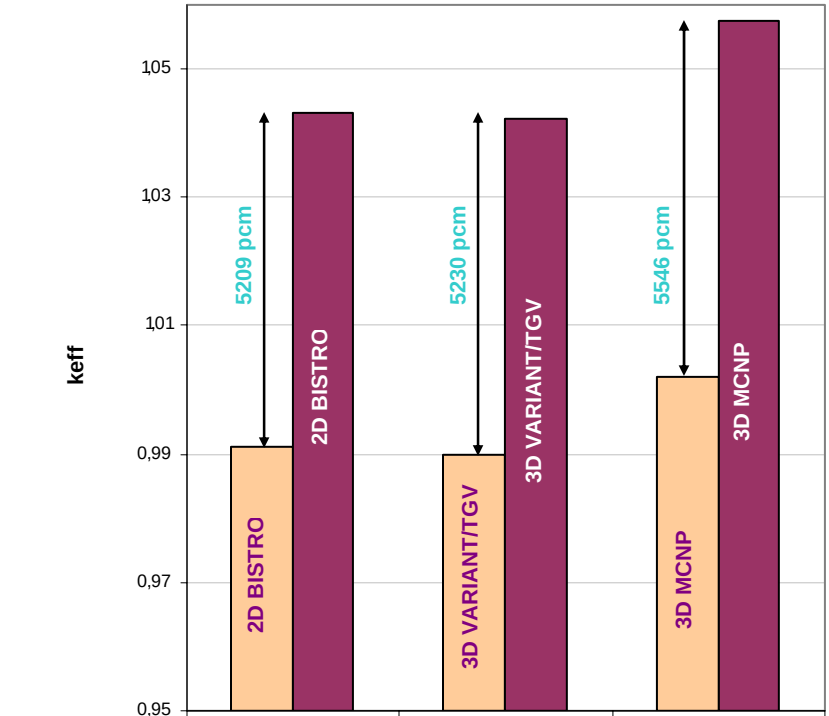


**Figure 7. ERANOS and MCNP results on $k_{eff}$ and $\Delta k_{eff}$.**

There are several possible sources of discrepancies in the $S_N$ and nodal calculations, such as the multigroup cross sections, the multidimensionality effect, the discretization errors in spatial and angular meshes, and the choice of various numerical alternatives.

Hence several ERANOS calculations have been carried out with different combinations of input options in order to investigate their effects.
It has been noticed that the Legendre expansion truncation accounts for some decades pcm: for instance, a $P_1$ treatment in the case of full TGV nodal solution/coarse mesh, causes a decrease of 40 pcm with respect to a $\Delta k$ estimation of 5423 pcm obtained with $P_{0\text{-corrected}}$.
In the same way, an approximate spherical harmonics treatment and a coarse mesh geometry description, associated with a $P_1$ Legendre expansion order, leads to values of $\Delta\rho$ more accordable to MCNP results ($\Delta\rho$ = 5171 pcm). An exact TGV resolution (instead of approximate) causes a reduction in the void reactivity worth to $\Delta\rho$= 5147 and a mesh refinement causes an additional decrease of about 80 pcm.
Nevertheless, the different deterministic $\Delta\rho$ (void effect) predictions appear to be quite consistent with the MCNP calculations: the discrepancy between the value obtained averaging the five deterministic results and the reference Monte Carlo is only ~2% and is probably due to the fact that the stochastic code is based on a point-wise representation of both cross sections and geometry, avoiding possible inconsistencies in generating condensed group cross sections and spatial dependence on homogenization and meshing.
Despite this and some other unresolved issues related to a precise comparison between ERANOS and MCNP outcomes, the accuracy of deterministic solutions and the deterministic/stochastic consistency at this stage are quite satisfactory from the viewpoint of $\Delta\rho$, i.e. the void reactivity worth.

## 5.3 Void Significant Parameters

The amount of reactivity void effect is due to many factors.
The effective multiplication factor is defined as follows:

$$k_{eff} = \frac{productions}{disappearences + leakage}. \tag{3}$$

In order to maintain coherence with the outcomes of the reference stochastic evaluations, (*n,xn*)-reactions have been neglected and only neutrons produced by fissions, captures and leakage have been considered as $k_{eff}$ contributors so that:

$$k_{eff} = \frac{\bar{\nu}\Sigma_f}{\Sigma_f + \Sigma_c + leakage}. \tag{4}$$

Accordingly,
$$\partial k_{eff} = f(\partial\bar{\nu}, \partial\Sigma_f, \partial\Sigma_a, \partial l) \tag{5}$$

$$\frac{\partial k_{eff}}{k_{eff}} = \frac{\partial\bar{\nu}}{\bar{\nu}} + \frac{\partial\Sigma_f}{\Sigma_f} - \frac{\partial\Sigma_a}{\Sigma_a}\cdot\frac{\Sigma_a}{\Sigma_a + l} - \frac{\partial l}{l}\cdot\frac{l}{\Sigma_a + l}, \tag{6}$$

where absorptions mean fissions plus captures.
Fission, capture and leakage 'reactions' have been normalized to the total number of events neutrons can undergo, in order to handle probabilities instead of reaction rates, as to comply with Monte Carlo results, which are source-neutron normalized.
After such a normalization, $k_{eff}$ denominator becomes equal to unity and therefore just the first two terms of (6) contribute to the void reactivity worth.
In Figure 8 the value of the average number of neutrons produced per fission $\bar{\nu}$, which depends only on the neutron spectrum, is plotted before and after occurrence of void.

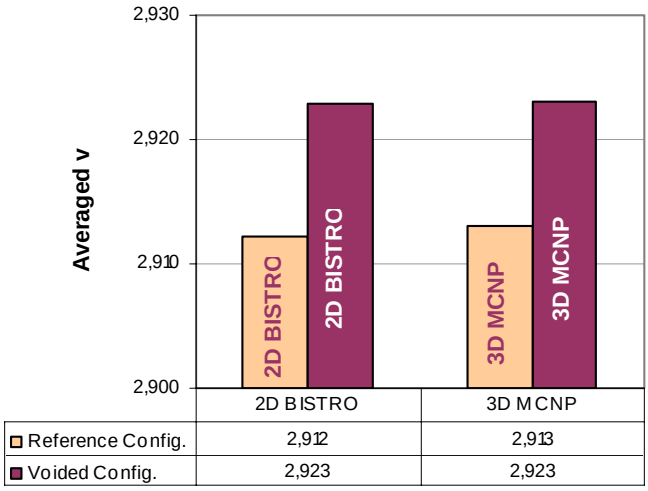


**Figure 8. Deterministic (2D-BISTRO calculation) and Monte Carlo estimation of the average number of neutrons produced per fission before and after core voiding.**

The effective multiplication factor is better explored in Figure 9, where each one of its components is plotted before and after occurrence of void.

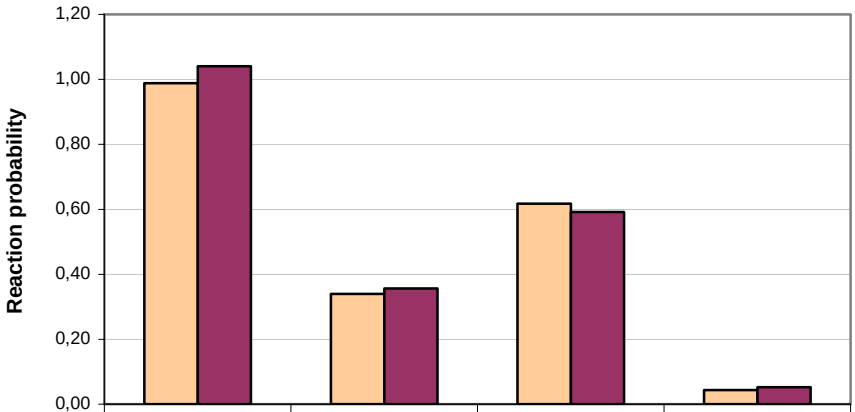


| | fission source | fission probability | capture probability | leakage probability |
|---|---|---|---|---|
| Reference Config. | 9,88E-01 | 3,39E-01 | 6,17E-01 | 4,38E-02 |
| Voided Config. | 1,04E+00 | 3,56E-01 | 5,91E-01 | 5,26E-02 |

**Figure 9. Reaction probabilities before and after core voiding (2D-BISTRO calculation).**

Excluded the approximation adopted in $k_{eff}$ evaluation, on the basis of the mentioned elaboration, the rise in reactivity appears to be due to the increase in both fission probability and $\bar{\nu}$. In fact, the averaged deterministic results show that the contribution of $\bar{\nu}$ relative variation accounts for about 340 pcm, with a very good agreement with Monte Carlo evaluation (1% discrepancy). Similarly, the relative variation of fission probabilities (obtained once more averaging deterministic calculations) have an impact of the order of 5000 pcm on $\partial k_{eff} / k_{eff}$ (Figure 10). The discrepancy with MCNP evaluations is around 3%.

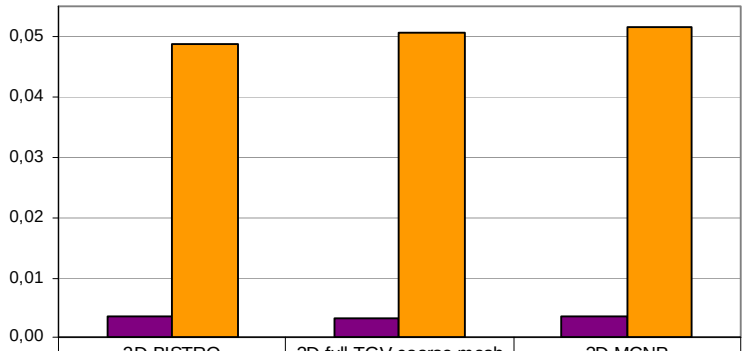


| | 2D BISTRO | 3D full TGV coarse mesh | 3D MCNP |
|---|---|---|---|
| Dnu/nu | 3,66E-03 | 3,26E-03 | 3,43E-03 |
| Dfission/fission | 4,87E-02 | 5,06E-02 | 5,17E-02 |

**Figure 10. Fission probability and $\bar{\nu}$ relative variation after voiding.**

As to leakage, a significant relative increase in its probability is observed. This effect is due to the fact that the system is more 'transparent' after voiding so that neutrons can escape more

efficiently because of a macroscopic absorption cross section global diminution. This is determined by a decrease of both material density (lack of coolant) and microscopic absorption cross section: neutrons interact with less atoms in the core and less efficiently as well, in absolute terms. In fact, results show that both fissions and captures diminish after voiding. Nevertheless, leakage negative contribution to the void effect is an order of magnitude smaller than positive contributions, so that it cannot balance the big positive reactivity worth.
Exploring absorptions into detail, an imbalance between fissions (positive contribution to void reactivity worth) and captures (negative contribution) occurs. The total macroscopic fission cross section decreases by ~6%, as a consequence of the predominance of odd-number actinides contributions, while the total macroscopic capture cross section undergoes an even larger diminution (~10%). Consequently, fission probability results enhanced despite the absolute diminution of the atoms intrinsic predisposition to fission, leading to a considerable $k_{eff}$ increase. As a confirmation, the ratio $\sigma_f / \sigma_a$ is heightened after voiding for each nuclide (Table I).

**Table I. Ratio of fission to absorption cross section before and after void occurrence.**

| Isotope | $\sigma_f / \sigma_a$ (reference core) | $\sigma_f / \sigma_a$ (voided core) |
|---|---|---|
| $^{234}$U | 0.332 | 0.370 |
| $^{235}$U | 0.775 | 0.781 |
| $^{236}$U | 0.163 | 0.205 |
| $^{238}$U | 0.102 | 0.144 |
| $^{238}$Pu | 0.691 | 0.709 |
| $^{239}$Pu | 0.777 | 0.792 |
| $^{240}$Pu | 0.410 | 0.456 |
| $^{241}$Pu | 0.839 | 0.843 |
| $^{242}$Pu | 0.324 | 0.372 |

## 5.4 Single Nuclides Contributions to the Void Reactivity Worth

In this section variation of fissions, captures (being escapes necessarily their complement) and $\nu$ due to voiding is investigated for each significant isotope composing the fuel, core-widely and for each enrichment core zone.
It can be observed once more that the main contribution to the void worth is an increase of fission probability of 'even-even' actinides.

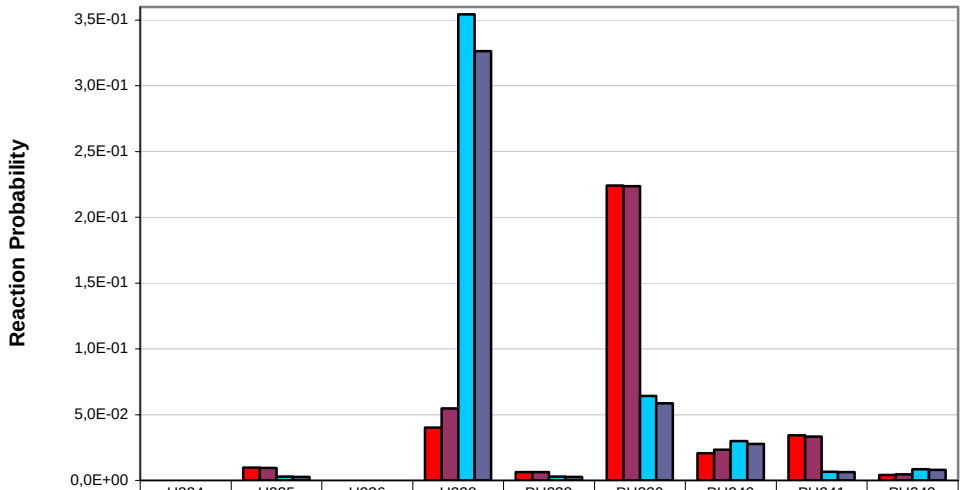


| | U234 | U235 | U236 | U238 | PU238 | PU239 | PU240 | PU241 | PU242 |
|---|---|---|---|---|---|---|---|---|---|
| Reference Fission Probability | 1,08E-05 | 9,68E-03 | 1,03E-05 | 4,02E-02 | 6,29E-03 | 2,24E-01 | 2,08E-02 | 3,42E-02 | 4,07E-03 |
| Voided Fission Probability | 1,23E-05 | 9,46E-03 | 1,30E-05 | 5,48E-02 | 6,43E-03 | 2,24E-01 | 2,33E-02 | 3,34E-02 | 4,71E-03 |
| Reference Capture Probability | 2,16E-05 | 2,81E-03 | 5,29E-05 | 3,54E-01 | 2,81E-03 | 6,42E-02 | 2,98E-02 | 6,56E-03 | 8,52E-03 |
| Voided Capture Probability | 2,10E-05 | 2,66E-03 | 5,04E-05 | 3,26E-01 | 2,64E-03 | 5,88E-02 | 2,79E-02 | 6,23E-03 | 7,96E-03 |

**Figure 11. Fission and capture probability breakdown by fuel nuclides (2D-BISTRO results).**

In Figure 11 fission and capture probabilities related to every single isotope composing the fuel have been plotted with regard to the reference and voided core.
It can be noticed that even-number isotopes of both uranium and plutonium undergo an increase in their fission probabilities.
On the contrary, odd-number isotopes show generally a reduction in their fission probabilities, yet less important than the even nuclides positive contribution.
Concerning capture probabilities, a uniform decreasing trend can be observed.
Uranium 238 plays the main role in the positive reactivity effect as a consequence of spectrum hardening: in particular, its overall contribution to $\partial k_{eff} / k_{eff}$ can be estimated to be of the order of 4320 pcm, which represents the summation of both contributions of its fission probability increase and average neutron number per fission raise (Figure 12).

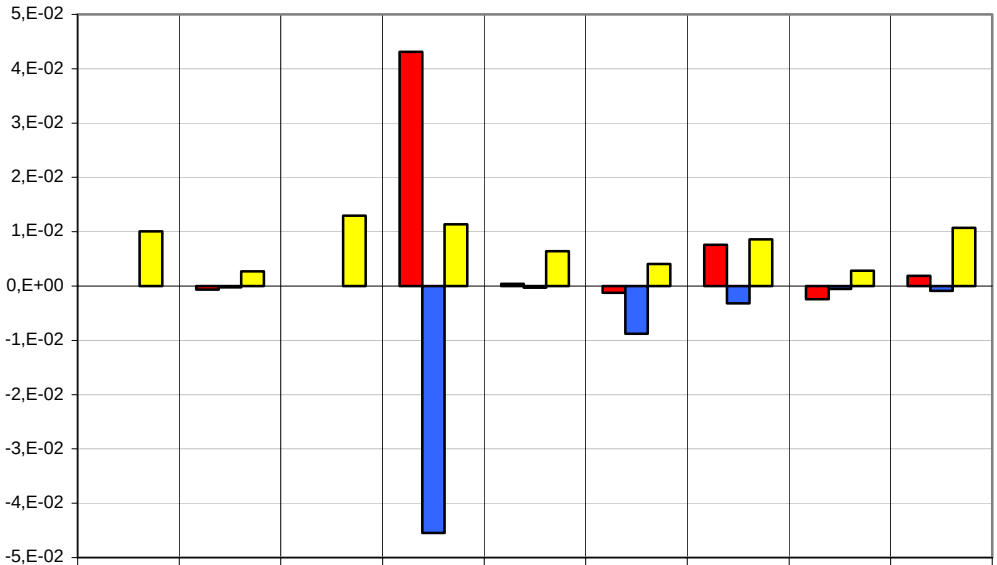


| | U234 | U235 | U236 | U238 | PU238 | PU239 | PU240 | PU241 | PU242 |
|---|---|---|---|---|---|---|---|---|---|
| deltaFISSION/FISSION | 4,56E-06 | -6,57E-04 | 7,90E-06 | 4,31E-02 | 4,03E-04 | -1,23E-03 | 7,57E-03 | -2,39E-03 | 1,89E-03 |
| deltaCAPTURE/CAPTURE | -1,01E-06 | -2,54E-04 | -4,11E-06 | -4,55E-02 | -2,80E-04 | -8,76E-03 | -3,19E-03 | -5,34E-04 | -9,03E-04 |
| deltaNU/NU | 1,01E-02 | 2,68E-03 | 1,30E-02 | 1,14E-02 | 6,43E-03 | 4,04E-03 | 8,61E-03 | 2,84E-03 | 1,07E-02 |

**Figure 12. Breakdown by nuclides of fission probability, capture probability and $\nu$ relative variation after voiding (2D-BISTRO).**

As to the latter, each isotope *i* contribution has been determined by expressing $\partial\bar{\nu}$ breakdown: starting from the definition

$$\bar{\nu} = \sum_i \nu_i \frac{F_i}{F_{tot}}, \tag{7}$$

$\partial\bar{\nu}/\bar{\nu}$ has been split into separate contributions:

$$\frac{\partial\bar{\nu}}{\bar{\nu}} = \frac{\sum_i \frac{\partial\nu_i}{\nu_i} F_i \nu_i}{\sum_i \nu_i F_i}, \tag{8}$$

where $F_i$ and $F_{tot}$ are the single isotope and the total fission probabilities respectively. Each nuclide relative variation of $\partial\nu$ is weighted by the ratio of its own productions to the total production term. Nevertheless, the function $\partial\bar{\nu}$ exhibits a strongly non-linear trend due to a great variation of the weights before and after voiding for some nuclides, so that a first order approximation leads to an overestimation of the actual $\partial\bar{\nu}/\bar{\nu}$. Consequently, a corrective factor has been applied to each isotope weight factor on the basis of its fission probability variation, and a rough estimation of its contribution to the void reactivity worth has been finally done.

As to uranium 238, its contribution to $\partial\bar{\nu}/\bar{\nu}$ is estimated around 9 pcm.

## 5.5 Single Nuclides Contributions for Each Enrichment Zone

For each enrichment zone fission and capture rates characterizing every single isotope composing the fuel have been plotted with regard to the two opposite contexts, before and after occurrence of void (Figure 13).

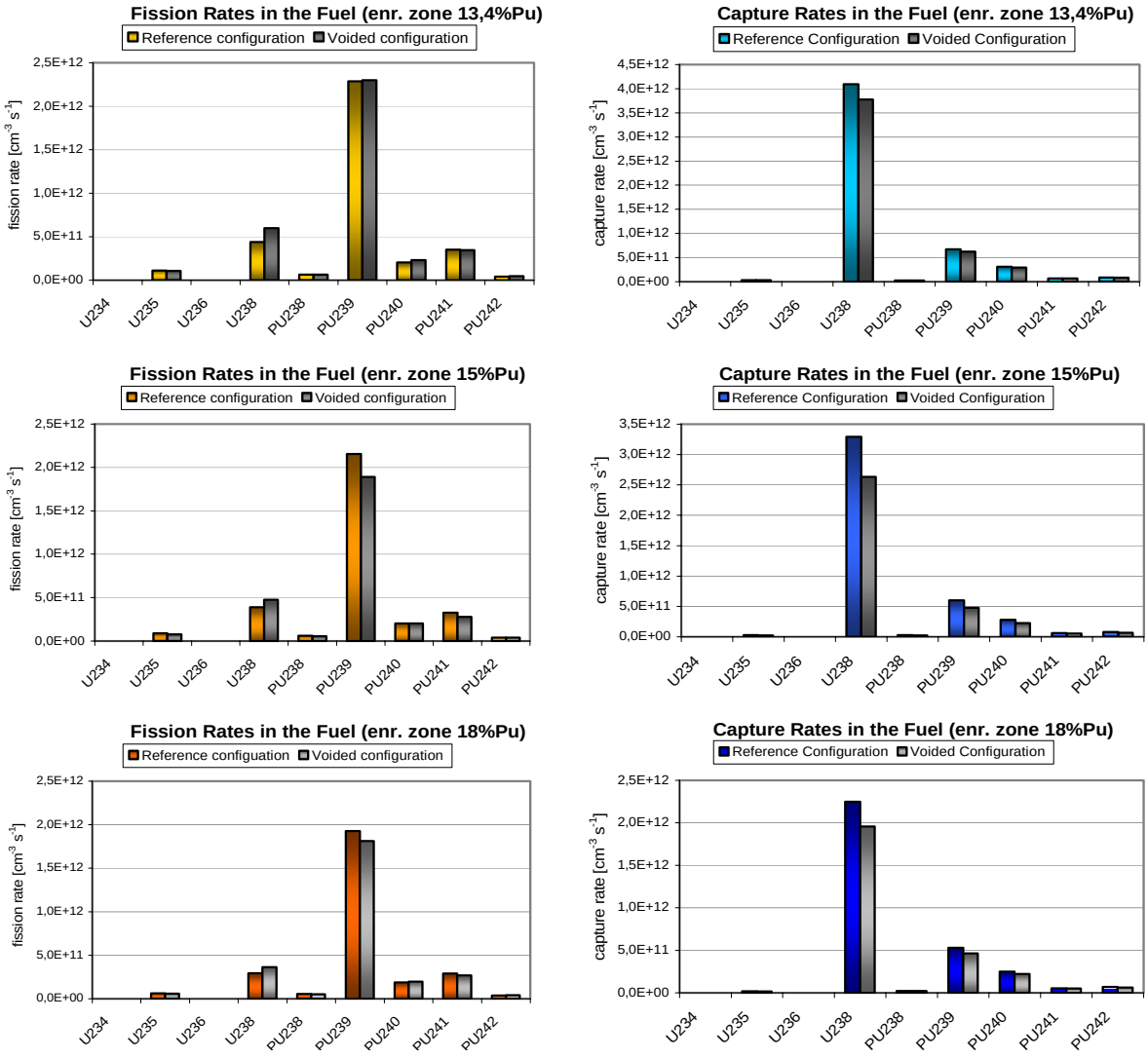


**Figure 13. Left column: fission rates. Right column: capture rates (2D-BISTRO).**

At a glance, a slight decrease of fission rates associated with a more significant reduction of capture rates is observable. The combination of these concurrent effects results in a positive contribution to the total void reactivity worth. In particular, the inner zone exhibits a small increase of fission rates associated with a considerable decrease of capture rates. The other two zones are characterized by relative diminution of both fission rates ($\propto 10^{-2}$) and capture rates ($\propto 10^{-1}$). A progressively smaller compensation between fissions slight decrease and major captures decrease is observable while moving toward the core periphery, as well as Monte Carlo results clearly show.

Despite the difficulty in inferring the contributions of each region to the void reactivity worth (many variables are playing together, namely the neutron flux radial distribution and the neutron spectrum), it is evident that the inner zone plays a foremost role to the positivity of the effect, while the intermediate and the outer zones give a gradually minor contribution.
A perturbative calculation has been carried out and results have confirmed the inner core importance to the void effect: its overall contribution accounts for about 4000 pcm, while the intermediate and the outer zones are responsible for a thousand and nearly zero pcm respectively.

As to different nuclides, the weight of uranium 238 in void effect is predominant in each enrichment zone.
Concerning the isotope plutonium 239, after voiding its fission rate is reduced in the second and in the third zone, while its contribution to void reactivity effect turns out to be slightly positive in the first one, in very good accordance with MCNP predictions.

As to the average number of neutrons per fission, an increase is observed for each fuel isotope in each core region. In particular, the intermediate enrichment zone is characterized by the largest increase of this parameter, followed by the inner and then by the outer one.
Uranium 236 undergoes the largest increase in $\nu$ in each zone, but its overall contribution to the void reactivity worth is almost negligible because of its scarcity. Uranium 238 comes immediately after and it is followed by the other even-number nuclides, as Figure 14 clearly illustrates.

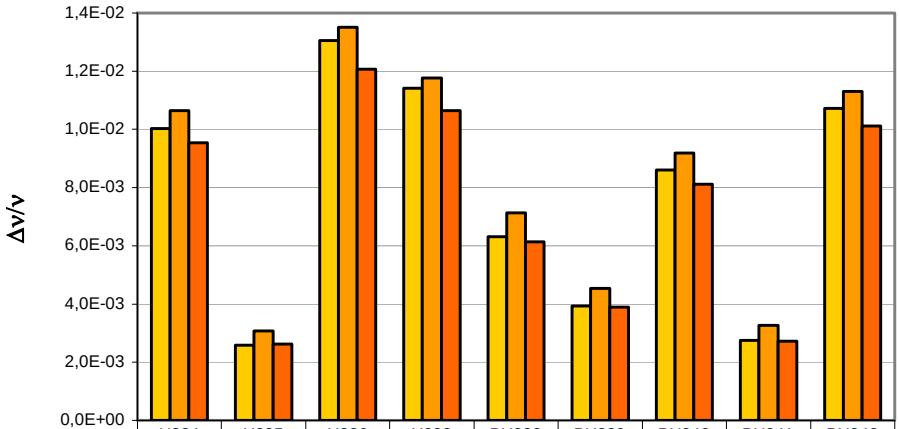


| | U234 | U235 | U236 | U238 | PU238 | PU239 | PU240 | PU241 | PU242 |
|---|---|---|---|---|---|---|---|---|---|
| Inner Fuel | 0,01003 | 0,00258 | 0,01305 | 0,01142 | 0,00631 | 0,00393 | 0,00861 | 0,00275 | 0,01073 |
| Intermediate Fuel | 0,01065 | 0,00308 | 0,01350 | 0,01178 | 0,00713 | 0,00453 | 0,00919 | 0,00327 | 0,01131 |
| Outer Fuel | 0,00953 | 0,00262 | 0,01207 | 0,01065 | 0,00613 | 0,00390 | 0,00811 | 0,00273 | 0,01011 |

**Figure 14. ν relative variation after voiding in each enrichment zone (2D-BISTRO).**

## 6. CONCLUSIONS

The purpose of this paper was the evaluation of the impact of a deterministic and stochastic approach on critical reactor parameters, and in particular on the actual void reactivity evaluation. The referring case was the preliminary core configuration of ELSY reactor.
The aim of the work was to outline the physical problem and to compare the values of calculated neutronic characteristics through a "cross-checked" analysis.

Firstly, the overall performance of the two different codes have been assessed by comparing predictions of the effective multiplication factor $k_{eff}$. Calculations carried out by means of ERANOS-2.1 code have shown that reactivity worth due to void effect in the active region is around 5100 pcm, with good agreement with MCNP-4a results (~5200 pcm).

Comparisons between the two approaches about different contributors show a general agreement on the main subject of the analysis. Both the approaches confirm:

- the huge positive void effect in the inner zone, decreasing toward the border of the active core, till becoming locally negative (inner zone: ~4000 pcm; intermediate zone: ~1000 pcm; outer zone: nearly zero);
- the predominant contributions of even isotopes to the void effect, among which uranium 238 plays a major role (~4300 pcm), because of their high sensitivity of fission cross-section to the spectrum hardening (threshold reactions), despite their modest contribution to the total fissions;
- the contribution of a few hundreds pcm (~340 pcm) by $\bar{\nu}$ because of the spectral hardening.

## REFERENCES

1. R.GHAZY, E. Padovani, M. E. Ricotti, C. Artioli, "ELSY Gen IV Lead Fast Reactor: Void Reactivity Effect Evaluation", *HLMC 2008 International Conference*, submitted & in press, Obninsk, September 2008.
2. M. SALVATORES et al., "Nuclear data needs for Advanced Reactor Systems. A NEA Nuclear Science Committee Initiative", *Proc. Int. Conf. ND-2007*, Nice, April 2007.
3. C. ARTIOLI, M. Sarotto, S. Massara, "Open Square Fuel Assembly design and drawings - Preliminary ELSY core design", Report Deliverable D6, FPN-P9IX-004, 2007.
4. ERANOS 2.1 Code Documentation.